Macromolecular Research, Vol. 22, No. 4, pp 412-417 (2014)
DOI 10.1007/s13233-014-2063-4

www.springer.com/13233
pISSN 1598-5032 eISSN 2092-7673

Development of pH-Responsive Chitosan-Coated Mesoporous Silica Nanoparticles

Muhammad Gulfam[1] and Bong Geun Chung*[,2]

[1]*Department of Bionano Technology, Hanyang University, Gyeonggi 426-791, Korea*
[2]*Department of Mechanical Engineering, Sogang University, Seoul 121-742, Korea*

Received October 5, 2013; Revised December 23, 2013; Accepted January 3, 2014

Abstract: We synthesized pH-responsive chitosan-coated mesoporous silica nanoparticles. The morphological characterization conveyed that the mesoporous silica was encapsulated within pH-responsive cationic chitosan. Further, the average diameter of chitosan-coated mesoporous silica nanoparticles was approximately 230 nm. The doxorubicin, an anticancer drug, was loaded into the cavities of mesoporous chitosan-coated silica nanoparticles. pH played an important role in regulating the release of doxorubicin from chitosan-coated mesoporous silica nanoparticles, indicating that 53% and 90% doxorubicin were released from chitosan-coated mesoporous silica nanoparticles within 48 h at pH 7.4 and pH 4.4, respectively. We also demonstrated the endocytosis of chitosan-coated mesoporous silica nanoparticles in MCF-7 breast cancer cells. Therefore, this chitosan-coated mesoporous silica nanoparticle could be a powerful tool for pH-responsive controlled release of the anticancer drug.

Keywords: pH-responsive chitosan, mesoporous silica nanoparticle, anticancer drug, controlled release.

Introduction

Stimuli-responsive polymers exhibit a dramatic and reversible phase change.[1-3] Stimuli-responsive smart polymers have great potential for applications in drug delivery, tissue engineering scaffold development, and biosensing.[2] In particular, silica nanoparticles with mesoporous surfaces are of great interest in applications of drug delivery due to their biocompatibility, large surface area, and tunable pore size.[4-6] Given these properties, mesoporous silica nanoparticles have been used for drug and gene delivery, cell imaging, and cancer therapy applications.[7-12] Despite the therapeutic effect of anticancer drug-loaded mesoporous silica nanoparticles, it has been known that nanocarriers might cause hemolysis and cytotoxicity.[4,13] *In vitro* toxicity of silica nanoparticles in human lung cancer cells has been investigated.[14] The cell viability was found to decrease in response to nanoparticle dosages and exposure times. Silica nanoparticles also increased levels of total reactive oxygen species (ROS) and reduced levels of glutathione. It has also been reported that silica nanoparticles might cause cytotoxicity and mitochondrial damage.[15] The nanoparticle-induced oxidative stress played an important role in regulating the apoptosis. It indicated that apoptosis through mitochondrial pathway was caused by silica nanoparticles. Furthermore, the cytotoxicity of silica nanoparticles in human endothelial cells has been reported.[16] The monodisperse silica nanoparticles with various sizes were synthesized and the effect of particle sizes on viability of endothelial cells was investigated that silica nanoparticles might cause cytotoxic damage. It has been demonstrated that small mesoporous silica nanoparticles (14-16 nm in diameter) caused cytotoxicity. In contrast, large mesoporous silica nanoparticles (104-335 nm in diameter) showed low cytotoxic response compared to small mesoporous silica nanoparticles, suggesting that the surface area of the nanoparticles would play an important role in determining the toxicity.

To overcome limitations of cytotoxicity and hemolysis caused by silica nanoparticles, the stimuli-responsive controlled release systems have previously been developed. Various strategies have been used to functionalize the surface of mesoporous silica nanoparticles. For instance, polyethyleneimine-coated mesoporous silica nanoparticles have been developed to enhance the cellular uptake and delivery of small interfering ribonucleic acid (siRNA) and deoxyribonucleic acid (DNA) constructs.[17] The non-covalent attachment of polyethyleneimine polymers increased cellular uptakes of mesoporous silica nanoparticles due to cationic surface to which DNA and siRNA constructs could be attached. The controlled release of molecules from mesoporous silica nanoparticles using poly(4-vinyl pyridine) (PVP) has also been reported.[18] The mesoporous silica was reacted with bromomethyldimethylchlorosilane to synthesize bromo-functionalized mesoporous silica. Subsequently, PVP was grafted to silica surfaces through quaternized pyridine groups, forming tethered polymer layers on the surface of mesoporous silica nanoparticles. It showed that the deprotonation of the poly-

*Corresponding Author. E-mail: bchung@sogang.ac.kr

mer at high pH produced a hydrophobic state and inhibited the release of molecules. In contrast, the swollen state of the protonated PVP was permeable to molecule transport at low pH. Moreover, the mesoporous silica nanoparticle-based lipid bilayer has been used as a target delivery of multicomponent cargos to cancer cells.[10] The protocells were loaded with combinations of doxorubicin, siRNA, and diagnostic agents (*e.g.*, quantum dots). They were modified to enhance endosomal escape and nuclear accumulation of selected cargos. The large capacity of the high-surface-area nanoporous core combined with the antitumor agent to increase target efficiency.

pH-responsive chitosan-based drug delivery systems[19] or chitosan-silica nanoparticles loaded with tumor necrosis factor-alpha (TNF-α) drugs[20] have previously been developed. Chitosan has widely been used for various biomedical applications and drug delivery systems due to its biocompatible properties.[3,21] It has previously been reported that the chitosan could be responsive to external pH, because the amino groups in chitosan were protonated at acidic pH. Therefore, the chitosan could be responded by slightly acidic pH, because pK_a of chitosan was approximately 6.3.[22] Despite recent development of silica and chitosan-silica hybrid nanoparticles, mesoporous silica nanoparticles coated with pH-responsive chitosan and loaded with doxorubicin anticancer drugs have not yet fully elucidated for endocytosis and controlled release applications of MCF-7 breast cancer cells. Here, we created pH-responsive chitosan-coated mesoporous silica nanoparticles. The anticancer drug (*e.g.*, doxorubicin) was loaded into the cavities of chitosan-coated mesoporous silica nanoparticles. The release of doxorubicin was regulated by pH, showing that doxorubicin was largely released from chitosan-coated mesoporous silica nanoparticles at acidic pH. Confocal microscopy images also showed endocytosis of chitosan-coated mesoporous silica nanoparticles in MCF-7 breast cancer cells. Therefore, this doxorubicin-loaded chitosan-coated mesoporous silica nanoparticle could be a powerful tool for pH-responsive controlled release and tumor therapy applications.

Experimental

Materials. Cetyltrimethylammonium bromide (CTAB), aqueous ammonia (NH_4OH, 25-28%), hydrochloric acid (HCl, 36-38%), fluorescein isothiocyanate (FITC), tetraethyl orthosilicate (TEOS), (3-Aminopropyl) triethoxysilane (APTES), chitosan (MW=60,000-120,000), and doxorubicin hydrochloride were purchased from Sigma Aldrich. Acetic acid (CH_3COOH, 99.5%purity), ethyl alcohol (99.9% purity), and diethyl ether (99.5% purity) were purchased from Samchun Chemicals, Korea.

Synthesis of Bare Mesoporous Silica Nanoparticles. The hierarchical bare mesoporous silica nanoparticles were generated using an ammonia-based catalysis method under highly dilute and low surfactant conditions (Figure 1). TEOS was used as a silica source. The reaction was performed at room temperature using water, ethyl alcohol, and diethyl ether as co-solvents. The cetyl trimethyl ammonium bromide was used as a template and surfactant. The particle size was controlled by adjusting ammonia concentrations, TEOS volumes, and reaction temperatures. Typically, 0.8 mL ammonium hydroxide, 10 mL ethyl alcohol, and 20 mL diethyl ether were dissolved in 70 mL distilled water. 500 mg CTAB was introduced in this emulsion system and the mixture was vigorously stirred at 600 rpm for 30 min. Afterward, 2.5 mL TEOS was quickly added into the system and the mixture was vigorously stirred at 600 rpm for 4 h. The precipitate was collected by filtration, was washed with distilled water, and was then dried in air at 60 °C for 24 h. The CTAB template was removed by vigorously stirring the particles in a mixture containing 15 mL HCl and 120 mL ethyl alcohol at 70 °C for 24 h. To remove the template and maintain the hierarchical mesoporous morphology of silica nanoparticles, the nanoparticles were further calcinated at 600 °C for 12 h. Finally, the bare mesoporous silica nanoparticles were washed several times with distilled water and ethyl alcohol and were subsequently dried in air at 80 °C.

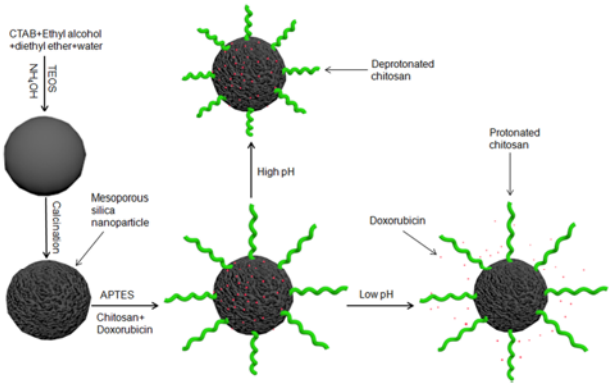

Figure 1. Schematics of controlled drug release from pH-responsive chitosan-coated mesoporous silica nanoparticles.

Synthesis of Chitosan-Coated Mesoporous Silica Nanoparticles. 25 mg chitosan was dissolved in 5 mL 3% acetic acid and the suspension was stirred at 600 rpm for 24 h to form chitosan solution (0.5% w/v) (Figure 1). 10 mg bare mesoporous silica nanoparticles were ultrasonicated in 5 mL ethyl alcohol for 10 min and the dispersion was adjusted to pH 3.5-4.5 by adding acetic acid. Subsequently, 200 μL APTES was added into the dispersion of bare mesoporous silica nanoparticles and was stirred for 4 h at room temperature. Finally, 5 mL of chitosan solution was added into the mixture of bare mesoporous silica nanoparticles and was subsequently stirred at room temperature for 24 h. The chitosan-coated mesoporous silica nanoparticles were collected by centrifugation at 10,000 rpm, following washing with excessive distilled water and ethyl alcohol before freeze-drying.

Doxorubicin-Loaded Chitosan-Coated Mesoporous Silica Nanoparticles. The doxorubicin was loaded into bare mesoporous silica and chitosan-coated silica nanoparticles. 10 mg bare mesoporous silica nanoparticles were dispersed in 5 mL of phosphate buffered saline (PBS) solution and were sonicated for 10 min. Afterward, 500 μg doxorubicin was added and the mixture was stirred at 600 rpm for 24 h. The doxorubicin-loaded bare mesoporous silica nanoparticles were collected by centrifugation at 10,000 rpm and the supernatant was used to measure the drug loading efficiency. The final product was washed with distilled water and was freeze-dried. To synthesize doxorubicin-loaded chitosan-coated mesoporous silica nanoparticles, 10 mg chitosan-coated mesoporous silica nanoparticles were dissolved using an ultrasonicator in 5 mL of PBS solution containing 500 μg doxorubicin and the mixture was stirred at 600 rpm for 24 h. Afterward, 0.2 M NaOH was added to adjust basic pH and the final product was collected by centrifugation at 10,000 rpm and the supernatant was analyzed to measure the drug loading efficiency. The doxorubicin-loaded chitosan-coated mesoporous silica nanoparticles were washed with PBS solution for several times, were centrifuged, and were then freeze-dried. The drug loading efficiency was calculated as follows: amount of drug in supernatant was divided by total amount of drug in system.

Morphological Analysis of Nanoparticles. The morphology of bare mesoporous silica and chitosan-coated mesoporous silica nanoparticles was analyzed by field emission scanning electron microscopy (FE-SEM). The nanoparticles were coated with platinum using a turbo sputter coater (EMITECH: K575X/Carb Peltier Cooled). The morphologies of bare mesoporous silica and chitosan-coated mesoporous silica nanoparticles were also analyzed by transmission electron microscopy (TEM, JEM-2100F).

Analysis of Nanoparticle Size and Zeta Potential. To analyze the size and charge, nanoparticles were dispersed in deionized water and were subsequently sonicated for 3 min. The size and charge of bare mesoporous silica and chitosan-coated mesoporous silica nanoparticles were analyzed by dynamic light scattering using a Zetasizer 4 (Malvern Instruments Ltd., UK). The charge of bare mesoporous silica and chitosan-coated mesoporous silica nanoparticles was analyzed by a laser-based multiple angle particle electrophoresis analyzer.

Drug Release Analysis. To analyze the doxorubicin released from bare mesoporous silica and chitosan-coated silica nanoparticles, the nanoparticles were dispersed in 10 mL of PBS solution at pH 4.4 and 7.4. The mixture was stirred at 100 rpm at 37 °C in a shaking incubator. 1 mL sample was drawn at different time intervals (1~48 h) and was replaced with 1 mL of PBS solution to maintain 10 mL volume. The sample was centrifuged at 1,000 rpm and the supernatant was analyzed to measure the controlled release of doxorubicin. The amount of doxorubicin released from bare mesoporous silica and chitosan-coated silica nanoparticles was calculated from a standard curve using a UV-visible spectrophotometer (Cary 100 UV-visible spectrophotometer) at 496 nm wavelength.

Results and Discussion

Synthesis and Characterization of Bare Mesoporous Silica Nanoparticles. The bare mesoporous silica nanoparticles were generated using cationic CTAB-template and NH_4OH catalyst under dilute aqueous conditions (Figure 1). CTAB was removed by extraction with HCl and calcinations to generate pores on the surface of bare silica nanospheres. The morphology of nanoparticles was characterized by FE-SEM (Figure 2(A)) and TEM analysis (Figure 2(C), (D)), showing spherical-shaped nanoparticles with hierarchical pores on the surface. The synthesis of bare mesoporous silica was based on formation of liquid-crystalline meso-phases of amphiphilic surfactant molecules that could serve as templates for *in situ* polymerization of orthosilicic acid. The synthesis could be performed in either acidic or basic conditions. The sodium silicate, fumed silica, and tetra-alkyl oxide of silane could be used as a source of silica. The synthesis of mesoporous silica required a template agent. The template directed the polymerization of silicates from a precursor (*e.g.*, an ester of orthosilicic acid) as previously described.[23] The particle size and morphology of mesoporous silica were controlled by hydrolysis rate, pH, condensation of the silica source, and magnitude of the interactions between the silica polymer and the assembled templates.

Synthesis and Characterization of Chitosan-Coated Mesoporous Silica Nanoparticles. Chitosan, a stimuli-responsive natural biopolymer, is a cationic polysaccharide composed by β-(1-4)-linked glucosamine units with *N*-acetyl-*D*-glucosamine.[3,19,21] We used chitosan to coat the surface of

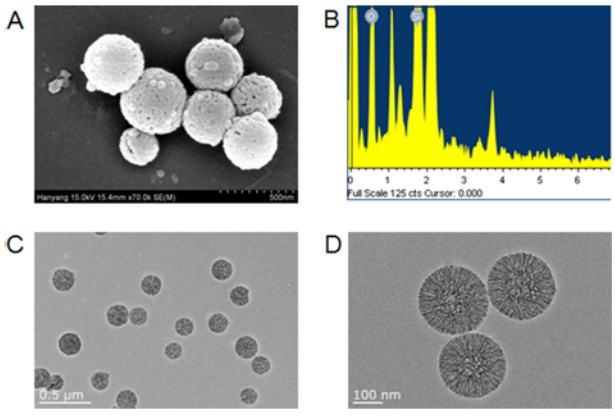

Figure 2. Morphological characterization of mesoporous silica nanoparticles. (A) FE-SEM image of mesoporous silica nanoparticles. (B) Elemental characterization of mesoporous silica nanoparticles. (C-D) TEM images of mesoporous silica nanoparticles.

SiO_2 to generate a pH-responsive polyelectrolyte layer (Figure 1). APTES was used to modify SiO_2 nanoparticles and was reacted with silanol groups on the SiO_2 surface to form Si-O-Si bonds. The chitosan solution was subsequently added to accomplish cross-linking on the surface of SiO_2 nanoparticles.[22] The morphology of SiO_2 nanoparticles containing chitosan layers was investigated by FE-SEM and TEM analysis (Figure 3). Elemental characterization showed Si, N, O, and C in chitosan-coated mesoporous silica nanoparticles (Figure 3(B)). The dynamic light scattering and zeta potential were also employed to analyze the size and charge of chitosan-coated mesoporous silica nanoparticles. It showed that the size of monodispersed chitosan-coated silica nanoparticles (230±13.5 nm in diameter) was larger compared to bare silica nanoparticles (225±7.2 nm in diameter). The zeta potential measurement represented that SiO_2 nanoparticles showed a negative potential (-2.67 mV), whereas the zeta potential of the chitosan-coated mesoporous silica nanoparticles increased to 2.79 mV due to the cationic polysaccharide chitosan. As a result, we confirmed that chitosan was coated on the SiO_2 nanoparticles.

Controlled Release of Anticancer Drug. The mesoporous silica was used as a carrier for drug delivery applications. The surface functionalization of silica was employed to enhance the interaction between drugs and nanoparticles. However, the release rate from surface-functionalized silica was not significantly different from the release rate of the bare silica. It has been reported that non-phagocytic eukaryotic cells could uptake particles as large as 500 nm in size and the uptake efficiency increased in particles around 200 nm or smaller,[24] suggesting that our nanoparticles could be potentially useful for drug delivery applications. The biocompatible polymer-coated nanoparticles are of great interest in regulating the delivery and controlled release of drugs.[25] We used doxorubicin, an anticancer drug, to analyze pH-dependent controlled release from bare mesoporous silica and chitosan-coated silica nanoparticles. Various parameters (*e.g.*, particle size, degradation rate, molecular weight, wettability, and binding affinity between the polymer and drug) play an important role in controlling the drug release.[26] Before the release analysis of anticancer drugs on nanoparticles, we measured the drug loading efficiency, showing that the low drug loading efficiency (68.93%) was observed at acid pH. In contrast, higher drug loading efficiency (83.23%) was observed at basic pH. We further quantified the concentration of doxorubicin released from mesoporous silica and chitosan-coated silica nanoparticles. We observed a rapid release (28%) of doxorubicin from mesoporous silica nanoparticles at pH 7.4 after 1 h compared to the chitosan-coated mesoporous silica nanoparticles (15%) (Figure 4(A)). At pH 7.4, 85% doxorubicin was released from bare mesoporous silica nanoparticles within 48 h. In contrast, slow drug release (53%) was observed in chitosan-coated mesoporous silica nanoparticles at pH 7.4 within 48 h. This slow drug release was attributed to the chitosan coated on the surface of mesoporous silica nanoparticles, because the chitosan chains were deprotonated at pH 7.4

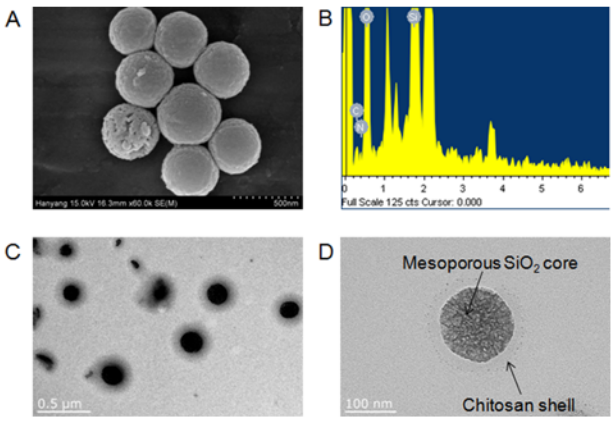

Figure 3. Morphological characterization of chitosan-coated mesoporous silica nanoparticles. (A) FE-SEM image of chitosan-coated silica nanoparticles. (B) Elemental characterization of chitosan-coated mesoporous silica nanoparticles. (C-D) TEM images of chitosan-coated mesoporous silica nanoparticles.

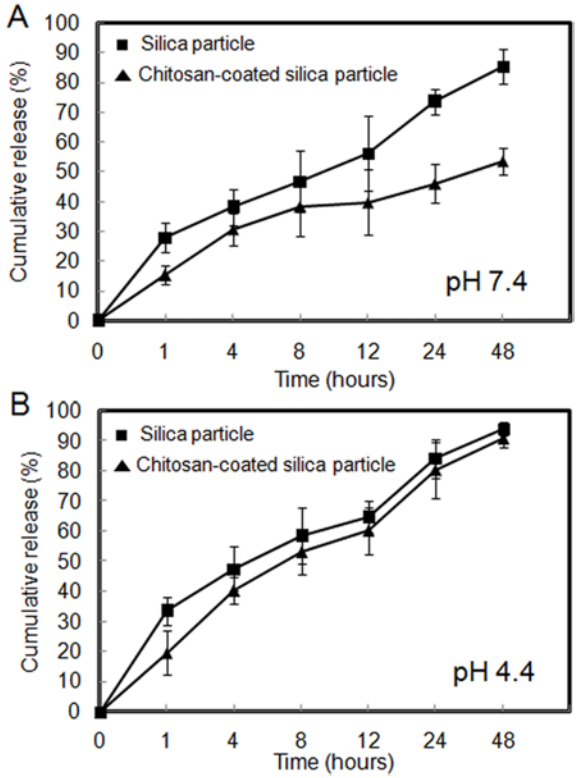

Figure 4. Analysis of doxorubicin released from mesoporous silica and chitosan-coated silica nanoparticles at (A) pH 7.4 and (B) pH 4.4. The drug release experiments were performed three times. All data are represented as means and error bars indicate the standard deviation.

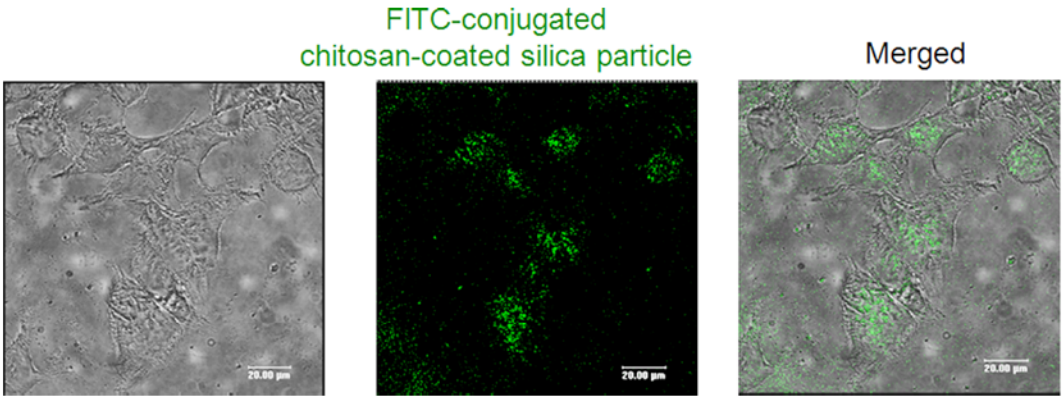

Figure 5. Confocal microscopy images of cellular uptake in MCF-7 breast cancer cells using FITC-loaded chitosan-coated mesoporous silica nanoparticles.

and were collapsed to close the pores on the chitosan-coated mesoporous silica nanoparticles. In contrast, chitosan-coated mesoporous silica nanoparticles released higher amounts (90%) of doxorubicin at pH 4.4 within 48 h (Figure 4(B)), because doxorubicin molecules were encapsulated inside the hollow nanospheres and were also absorbed by the chitosan layers due to the positive charge and amino functional group on the surface as previously described.[27] At acidic pH, the cationic chitosan chains were protonated and were also swelled to open the pores of the chitosan-coated mesoporous silica nanoparticles as previously described.[3,20] The different behavior of doxorubicin release at different pH could be affected by collapse and swelling of the chitosan layers on the surface of the silica nanoparticles. As a result, pH-responsive chitosan plays an important role in controlling the drug release. To confirm the endocytosis of chitosan-coated mesoporous silica nanoparticles in MCF-7 breast cancer cells, we further investigated the cellular uptake of fluorescein isothiocyanate (FITC)-conjugated chitosan-coated mesoporous silica nanoparticles (Figure 5). Confocal microscopy images showed that FITC-conjugated chitosan-coated mesoporous silica nanoparticles were localized in cytosol of MCF-7 breast cancer cells. It revealed that cancer cells containing FITC-conjugated chitosan-coated mesoporous silica nanoparticles were highly viable after cellular uptake. It has been known that the microenvironment in tumor tissues is acidic compared to normal tissues (*e.g.*, pH 7.4) as previously described.[28] The chitosan-coated mesoporous silica nanoparticles released 90% doxorubicin in acidic medium (pH 4.4), whereas 53% drug was released from chitosan-coated mesoporous silica nanoparticles at pH 7.4. It suggests that anticancer drugs on chitosan-coated mesoporous silica nanoparticles could be highly released at acidic tumor tissues, whereas drug release behavior might be negligible at normal tissues. Therefore, pH-responsive chitosan-coated mesoporous silica nanoparticles could be clinically useful for *in vivo* tumor therapy applications.

Conclusions

We synthesized silica nanoparticles with hierarchical mesopores on the surface. The surface of mesoporous silica nanoparticles was functionalized with amino group and the chitosan was subsequently grafted on the surface of mesoporous silica nanoparticles. The anticancer drug (*e.g.*, doxorubicin) was loaded into the bare mesoporous silica and chitosan-coated silica nanoparticles. We demonstrated that doxorubicin was slowly released from chitosan-coated mesoporous silica nanoparticles at pH 7.4. In contrast, doxorubicin was rapidly released from chitosan-coated mesoporous silica nanoparticles at pH 4.4 due to pH-sensitivity of chitosan. The confocal microscopy images demonstrated endocytosis of chitosan-coated mesoporous silica nanoparticles in MCF-7 breast cancer cells Therefore, this chitosan-coated mesoporous silica nanoparticle could be a potentially powerful carrier for pH-responsive controlled release of anticancer drugs.

Acknowledgments. This paper was supported by Basic Science Research Program through the National Research Foundation of Korea (NRF) funded by the Ministry of Science, ICT and Future Planning (grant number 20110016331, 2012R1A1A2005822). This work was also supported by the Sogang University Research Grant of 2013 (Grant Number 201310012.01, SRF-201314004). We thank to Mr. Jong Min Lee for helping the cell culture and confocal microscope.

References

(1) P. S. Stayton, T. Shimoboji, C. Long, A. Chilkoti, G. Ghen, J. M. Harris, and A. S. Hoffman, *Nature*, **378**, 472 (1995).
(2) D. Roy, J. N. Cambre, and B. S. Sumerlin, *Prog. Polym. Sci.*, **35**, 278 (2010).
(3) N. Bhattarai, J. Gunn, and M. Zhang, *Adv. Drug Deliv. Rev.*, **62**, 83 (2010).
(4) Y. S. Lin and C. L. Haynes, *J. Am. Chem. Soc.*, **132**, 4834 (2010).
(5) I. I. Slowing, B. G. Trewyn, and V. S. Y. Lin, *J. Am. Chem.*

Soc., **129**, 8845 (2007).
(6) S. C. Warren, F. J. DiSalvo, and U. Wiesner, *Nat. Mater.*, **6**, 156 (2007).
(7) Y. Zhu, J. Shi, W. Shen, X. Dong, J. Feng, M. Ruan, and Y. Li, *Angew. Chem. Int. Ed.*, **44**, 5083 (2005).
(8) X. Jiang, T. L. Ward, Y. S. Cheng, J. Liu, and C. J. Brinker, *Chem. Commun.*, **46**, 3019 (2010).
(9) J. Zhu, J. Tang, L. Zhao, X. Zhou, Y. Wang, and C. Yu, *Small*, **6**, 276 (2010).
(10) C. E. Ashley, E. C. Carnes, G. K. Phillips, D. Padilla, P. N. Durfee, P. A. Brown, T. N. Hanna, J. Liu, B. Phillips, M. B. Carter, N. J. Carroll, X. Jiang, D. R. Dunphy, C. L. Willman, D. N. Petsev, D. G. Evans, A. N. Parikh, B. Chackerian, W. Wharton, D. S. Peabody, and C. J. Brinker, *Nat. Mater.*, **10**, 389 (2011).
(11) M. Gary-Bobo, O. Hocine, D. Brevet, M. Maynadier, L. Raehm, S. Richeter, V. Charasson, B. Loock, A. Morère, P. Maillard, M. Garcia, and J. O. Durand, *Int. J. Pharm.*, **423**, 509 (2012).
(12) S. H. Cheng, C. H. Lee, C. S. Yang, F. G. Tseng, C. Y. Mou, and L. W. Lo, *J. Mater. Chem.*, **19**, 1252 (2009).
(13) A. J. Di Pasqua, K. K. Sharma, Y. L. Shi, B. B. Toms, W. Ouellette, J. C. Dabrowiak, and T. Asefa, *J. Inorg. Biochem.*, **102**, 1416 (2008).
(14) W. Lin, Y. W. Huang, X. D. Zhou, and Y. Ma, *Toxicol. Appl. Pharm.*, **217**, 252 (2006).
(15) L. Sun, Y. Li, X. Liu, M. Jin, L. Zhang, Z. Du, C. Guo, P. Huang, and Z. Sun, *Toxicol. In Vitro*, **25**, 1619 (2011).
(16) D. Napierska, L. C. J. Thomassen, V. Rabolli, D. Lison, L. Gonzalez, M. Kirsch-Volders, J. A. Martens, and P. H. Hoet, *Small*, **5**, 846 (2009).
(17) T. Xia, M. Kovochich, M. Liong, H. Meng, S. Kabehie, S. George, J. I. Zink, and A. E. Nel, *ACS Nano*, **3**, 3273 (2009).
(18) R. Liu, P. Liao, J. Liu, and P. Feng, *Langmuir*, **27**, 3095 (2011).
(19) J. H. Jang, Y. M. Choi, Y. Y. Choi, M. K. Joo, M. H. Park, B. G. Choi, E. Y. Kang, and B. Jeong, *J. Mater. Chem.*, **21**, 5484 (2011).
(20) Z. Deng, Z. Zhen, X. Hu, S. Wu, Z. Xu, and P. K. Chu, *Biomaterials*, **32**, 4976 (2011).
(21) J. Wu, Z.-G. Su, and G.-H. Ma, *Int. J. Pharm.*, **315**, 1 (2006).
(22) J. Wu and M. J. Sailor, *Adv. Funct. Mater.*, **19**, 733 (2009).
(23) Y. Wan and D. Zhao, *Chem. Rev.*, **107**, 2821 (2007).
(24) J. Rejman, V. Oberle, I. S. Zuhorn, and D. Hoekstra, *Biochem. J.*, **377**, 159 (2004).
(25) M. Gulfam, J. Kim, J. M. Lee, B. Ku, B. H. Chung, and B. G. Chung, *Langmuir*, **28**, 8216 (2012).
(26) H. Ge, Y. Hu, X. Jiang, D. Cheng, Y. Yuan, H. Bi, and C. Yang, *J. Pharm. Sci.*, **91**, 1463 (2002).
(27) S. W. Song, K. Hidajat, and S. Kawi, *Chem. Commun.*, 4396 (2007).
(28) F. Danhier, O. Feron, and V. Préat, *J. Control. Release*, **148**, 135 (2010).